

# Effects of TiO<sub>2</sub>-SiO<sub>2</sub> fillers on thermal and dielectric properties of bismuth glass microcomposite dielectrics for plasma display panel

Anal Tarafder · Shiv Prakash Singh · Basudeb Karmakar\*

*Glass Science & Technology Section, Glass Division,  
Central Glass and Ceramic Research Institute,  
Council of Scientific and Industrial Research (CSIR, India),  
196, Raja S.C. Mullick Road, Kolkata 700 032, India*

---

**Abstract** The combined effects of TiO<sub>2</sub> and SiO<sub>2</sub> fillers on thermal and dielectric properties of a new lead-free environmental friendly zinc bismuth borate, ZnO-Bi<sub>2</sub>O<sub>3</sub>-B<sub>2</sub>O<sub>3</sub> (ZBIB) glass microcomposite dielectrics have been investigated from the viewpoint of application as rear glass dielectric layer of plasma display panels (PDPs). The interaction of fillers with glass occurred during firing has also been explored by XRD, SEM and FTIR spectroscopic analyses. All the properties are found to be regulated by the covalent character (a fundamental property) of resultant microcomposite dielectrics. In this work, the co-addition of TiO<sub>2</sub>-SiO<sub>2</sub> filler to ZBIB glass is found to be more effective to adjust the required properties to employ with PD200 glass substrate in PDP technology.

---

\* Corresponding author. Tel.: +91 33 2473 3496; fax: +91 33 2473 0957.

*E-mail address:* basudebk@cgcric.res.in (B. Karmakar).

# 1 Introduction

In the last decade, the commercial uses of flat panel displays (FPDs) have increased enormously, especially in case of consumer electronics such as televisions, laptop computers, digital clocks, cell phones, telephones etc. In such cases, the most widely used flat panel display is the liquid crystal display (LCD). But plasma display panels (PDP) which is one kind of flat panel display have emerged to be a potential display material for large dimension (> 100 inches) high definition TV. Significant quality differences remain between PDP and LCD while they offer some shared benefits. PDPs are characterized by larger screen sizes (greater than 100 inches), wide viewing angle, more accurate image reproduction with better colour accuracy, contrast and brightness, superior ability to display moving images without motion artifacts and better pixel reliability over LCDs [1]. In PDP a rear glass dielectric layer (popularly known as white back) is used as the insulating film of the address electrodes on the rear glass substrate and also gives mechanical support to the barrier ribs (the partitions between the phosphor cavities). White back materials of PDP systems require a low dielectric constant (less than 15), low softening temperature (less than the strain point of PDP glass substrate which is 610°C for PD200) and low coefficient of thermal expansion (less than  $83 \times 10^{-7}/K$ ) with respect to use of PD200 glass as substrate [1, 2]. Lead oxide (PbO) containing glass microcomposites (micron sized ceramic oxide reinforced glass) are being used as white dielectric layer of PDPs [1-6]. But recently, interest in Pb-free glass systems has greatly increased with regard to their application in white backs of plasma display panels due to hazardous effects of Pb on health and environment during processing and discarding [1, 2, 4-7].

Several studies have been carried out by adding various types of crystalline fillers (e.g.,  $\text{TiO}_2$ ,  $\text{SiO}_2$ ,  $\text{ZrO}_2$ ,  $\text{Al}_2\text{O}_3$ ,  $\text{MgO}$  and cordierite) to lead free  $\text{BaO-ZnO-B}_2\text{O}_3\text{-SiO}_2$  [2-4],  $\text{BaO-B}_2\text{O}_3\text{-SiO}_2$  [5] and  $\text{BaO-ZnO-B}_2\text{O}_3$  [6] glass systems where the behavior of the composites with respect to different properties have been reported for use in PDPs. Very recently, Chong et al. [8, 9] have examined the influence of  $\text{Al}_2\text{O}_3$ ,  $\text{TiO}_2$  and  $\text{ZrO}_2$  ceramic filler on the thermophysical and dielectric properties of  $\text{BaO-ZnO-B}_2\text{O}_3\text{-P}_2\text{O}_5$  glass composites for plasma display panels. In this work, we have tried to replace lead oxide,  $\text{PbO}$  (MP =  $880^\circ\text{C}$ ,  $n = 2.24$ ) [10] by bismuth oxide ( $\text{Bi}_2\text{O}_3$ ) because of its low melting temperature ( $820^\circ\text{C}$ ) and high refractive index ( $n = 2.5$ ). Above all  $\text{Bi}_2\text{O}_3$  is not as hazardous as  $\text{PbO}$  [7] and  $\text{Bi}_2\text{O}_3$  is being considered a suitable alternative of  $\text{PbO}$  with respect to environmental friendliness. So, attempts were made to incorporate  $\text{Bi}_2\text{O}_3$  in the glass composition. To the best of our knowledge, there is no report on the combined effects of  $\text{TiO}_2\text{-SiO}_2$  fillers on thermal and dielectric properties of bismuth containing glass with the view of its use as rear glass dielectric layer (white back) of plasma display panels.

In view of above, in this study we report the combined effect the  $\text{TiO}_2$  (crystalline, rutile) and  $\text{SiO}_2$  (amorphous, spherical) fillers to an extent of 25 wt% on the softening point ( $T_s$ ), glass transition temperature ( $T_g$ ), coefficient of thermal expansion (CTE) and dielectric constant ( $\epsilon_r$ ) of lead-free  $\text{ZnO-Bi}_2\text{O}_3\text{-B}_2\text{O}_3$  glass. Here,  $\text{SiO}_2$  having low CTE ( $5.5 \times 10^{-7}/\text{K}$ ), low  $\epsilon_r$  (3.8) and high  $T_s$  ( $1723^\circ\text{C}$ ); and  $\text{TiO}_2$  having high CTE ( $80\text{-}100 \times 10^{-7}/\text{K}$ ), high  $\epsilon_r$  (80-100) and high  $T_s$  ( $1850^\circ\text{C}$ ) have been selected for controlling CTE,  $\epsilon_r$  and  $T_s$  of the resultant microcomposite dielectrics. The glass-filler interaction which

occurs at the sintering temperature has also been investigated by XRD, SEM and FTIR spectral analyses.

## 2 Experimental

### 2.1 Preparation of glass and microcomposite dielectrics

The selected glass composition (wt%) is 19ZnO-46Bi<sub>2</sub>O<sub>3</sub>-35B<sub>2</sub>O<sub>3</sub> (ZBIB). We have selected this glass composition to meet the requirement of three important properties of plasma display panel such as (i) coefficient of thermal expansion, CTE (less than  $83 \times 10^{-7}/K$ ), (ii) dielectric constant (less than 15) and (iii) softening point,  $T_s$  (less than 580°C). The batch was prepared using the pure raw materials: ZnO (GR, 99%, Loba Chemie, Mumbai, India), Bi<sub>2</sub>O<sub>3</sub> (99%, Loba Chemie, Mumbai, India) and H<sub>3</sub>BO<sub>3</sub> (GR, 99.5%, Loba Chemie, Mumbai, India). About 600 g of glass was melted in a platinum crucible in an electrically heated raised hearth furnace at 1150°C for 1h in air with intermittent stirring. The molten glass was quenched by casting onto an iron plate. The quenched glass was initially crushed in a stainless steel mortar and then pulverized in a planetary ball mill (Model PM100, Retsch, Germany) using a zirconia jar and balls to obtain final glass powders of 14.4 μm size ( $d_{50}$ ).

The pulverized ZBIB glass powders were mixed in isopropanol medium with appropriate amount of microsilica (spherical), SiO<sub>2</sub> (99.5 %,  $d_{50} = 1.5 \mu\text{m}$ , Pooja Enterprises, Mumbai, India) and titania, TiO<sub>2</sub> (99.9 %,  $d_{50} = 3.2 \mu\text{m}$ , Sigma-Aldrich, St. Louis, MO) fillers in an agate mortar. All the powders were then granulated using 2 wt% aqueous solution of polyvinyl alcohol (PVA) followed by pressing uniaxially into disk or cylindrical shape under a pressure of 500 kgf/cm<sup>2</sup> and then dried. It was sintered at 560°C

for 2h in air for measurement of coefficient of thermal expansion, dielectric constant, XRD, SEM and FTIR spectra. The composition of microcomposites is listed in Table 1.

## 2.2 Characterization

Particle size analyses of powders were carried out using a particle size analyzer (Model Mastersizer 2000, Malvern Instrument, Worcestershire, UK). XRD data were recorded using an XPERT-PRO MPD diffractometer (PANalytical, Almelo, the Netherlands) with Ni-filtered and anchor scan parameter wavelength  $1.54060 \text{ \AA}$  ( $\text{CuK}\alpha$ ) at  $25^\circ\text{C}$  at 40 kV and 30 mA and a scan speed  $10^\circ/\text{min}$ . The morphology of the samples was investigated with a SEM (Model S 430i, LEO Electronic Microscopy Ltd., Cambridge, UK) instrument at an accelerating potential of 15 kV. FTIR spectra were recorded by dispersing the sintered glass and microcomposite dielectric powders in KBr with a FTIR spectrometer (Model 1615, Perkin-Elmer Corporation, Norwalk, CT) at a resolution of  $\pm 2 \text{ cm}^{-1}$  after 16 scans. It was calibrated with a polystyrene film supplied by the instrument manufacturer.

The softening point ( $T_s$ ) of the dried disk was measured by a glass softening point system (Model SP-3A, Harrop Industries Inc., OH) with an accuracy of  $\pm 1^\circ\text{C}$ . The instrument was previously calibrated with a NBS (National Bureau of Standards, USA) standard glass of known softening point. The CTE and  $T_g$  of the sintered microcomposite cylinders were measured with an accuracy of  $\pm 1\%$  using a horizontal-loading dilatometer (Model 402C, NETZSCH-Gerätebau GmbH, Germany) after calibration with a standard alumina supplied with the instrument by the manufacturer. The CTE in the temperature range  $50\text{-}350^\circ\text{C}$  is reported here. The dielectric constant was measured with an accuracy

of  $\pm 1\%$  at a frequency of 1MHz using a LCR meter (Model 3532-50 Hitester, Hioki, Ueda, Nagano, Japan) at 25°C. The instrument was calibrated previously by a Suprasil-W silica glass ( $\epsilon_r = 3.8$ ).

### **3 Results and discussion**

#### **3.1 Particle size distribution**

It is well known that the degree of glass-filler interaction (powders-solid state reaction) is largely depended on their particle size and its distribution. The smaller the particle sizes of the fillers, the greater the extent of interaction. Thus the particle size distribution of ZBIB glass powder, TiO<sub>2</sub> and SiO<sub>2</sub> fillers is measured and presented in Fig. 1. It is seen that the glass powder as well as TiO<sub>2</sub> and SiO<sub>2</sub> fillers exhibit a bimodal particle size distribution. Bimodal particle sizes are beneficial to obtain high packing density. The median particle sizes ( $d_{50}$ ) ZBIB glass powder, TiO<sub>2</sub> and SiO<sub>2</sub> fillers are found to be 14.4, 3.2 and 1.5  $\mu\text{m}$  respectively. The compositions of microcomposite dielectrics are given in Table 1.

#### **3.2 XRD analysis**

As the reaction of fillers (TiO<sub>2</sub> and SiO<sub>2</sub>) with glass during firing at 560°C is the fundamental to the formation of filler-glass microcomposites, thus they have been examined by XRD analysis. The variation of XRD patterns with added TiO<sub>2</sub>-SiO<sub>2</sub> filler content is shown in Fig. 2. ZBIB glass is X-ray amorphous (Fig. 2, curve a). Since the added SiO<sub>2</sub> filler is amorphous (see Fig. 2, curve f) so there is no XRD peak of SiO<sub>2</sub> whereas on the other hand TiO<sub>2</sub> filler is rutile (see Fig. 2, curve g), so the composite C1

containing highest  $\text{TiO}_2$  exhibits well developed XRD pattern of rutile  $\text{TiO}_2$  (JCPDS card file No.: 21-1276) with diminished amorphous character (see curve b). With gradual decrease in  $\text{TiO}_2$  content and increase in  $\text{SiO}_2$ , the characteristic peaks of rutile  $\text{TiO}_2$  decrease and amorphous character gradually increases. XRD pattern also indicates that the filler has partially dissolved in glass during sintering at  $560^\circ\text{C}$  leaving behind some residual filler in the glass matrix which exhibit their characteristic peaks. This observation correlates well with those of FTIR spectral study as discussed later. Thus, it is clear from XRD analysis that combined  $\text{TiO}_2$ - $\text{SiO}_2$  filler containing microcomposite dielectrics are of crystal (ceramic)-in-amorphous characteristics.

### **3.3 Microstructural analysis**

The SEM analysis of the sintered samples was performed by grinding and polishing followed by etching in 1% aqueous solution of HF for 60 s. The dried samples were examined after Au coating on the surface to pass the electron beam through it. The fact that the fillers have partially dissolved in the glass matrix during sintering is evidenced by SEM images of the microcomposite dielectrics as shown in Fig. 3 (a) and (b) of samples C1 and C4 respectively. They exhibit the porous microstructure which is beneficial and essential to anchor the red, green and blue (RGB) phosphors. They also show the distribution of fillers in the microcomposite dielectrics after sintering. It is seen from Fig. 3 (a) of composite C1 which contains 20%  $\text{TiO}_2$  and 5%  $\text{SiO}_2$  fillers that  $\text{TiO}_2$  is almost dissolved in the glass whereas a large number of small irregular spherical particles of  $\text{SiO}_2$  found to be embedded in the glassy matrix. It is seen that the degree of solubility of  $\text{TiO}_2$  is higher than that of  $\text{SiO}_2$ . The glassy matrix is distinctly visible here. However, the

picture is entirely different in Fig. 3 (b) of composite C4 which contains 5% TiO<sub>2</sub> and 20% SiO<sub>2</sub> fillers. Here it is seen that TiO<sub>2</sub> dissolves almost completely and SiO<sub>2</sub> fillers remain relatively undissolved. Thus partial solubility of the added filler in the glass matrix generates closed pores in the microcomposite dielectrics. As a result of the presence of undissolved SiO<sub>2</sub> and TiO<sub>2</sub> fillers with closed pores, the bulk density of resultant microcomposites decreases and the same is reflected in Fig. 4. This matter can easily be realized if one consider and compare the SEM images of microstructures of C1 and C4.

### 3.4 FTIR spectra analysis

The FTIR spectra of TiO<sub>2</sub>-SiO<sub>2</sub> containing microcomposite dielectrics are depicted in Fig. 5. The ZBIB glass exhibits three distinct bands around 1346, 954 and 685 cm<sup>-1</sup>, which are attributed to asymmetric stretching vibration of B-O-B bond of the trigonal [BO<sub>3</sub>] units, asymmetric stretching vibration of B-O-B bond of the tetragonal [BO<sub>4</sub>] units, and bending vibration of B-O-B linkages of the borate glass networks, respectively [11-13]. The band appeared at 685 cm<sup>-1</sup> is also due to the stretching vibration of Bi-O-Bi bond of [BiO<sub>6</sub>] octahedral [14, 15]. The SiO<sub>2</sub> filler also exhibits three intense bands at around 1115, 815 and 469 cm<sup>-1</sup> which are attributed to asymmetric stretching vibration of Si-O-Si bond, symmetric stretching vibrations of O-Si-O bond and bending vibration of Si-O-Si bond of [SiO<sub>4</sub>] tetrahedra respectively [11]. It is seen from Fig. 5 that with increasing SiO<sub>2</sub> filler in the composites C1 to C4 all these three bands gradually become more intense along with the intensity decrease and changes of the shape of all the three bands of the ZBIB glass. The bands at around 1238, 1100 and 923 cm<sup>-1</sup> are attributed to

asymmetric vibration of B-O-Si bond [11]. This fact clearly indicates the distinct interaction of ZBIB glass with SiO<sub>2</sub> filler.

The TiO<sub>2</sub> (rutile) filler, on the other hand, exhibits only one very strong doublet absorption band peaking at 654 and 546 cm<sup>-1</sup> which are due to stretching vibrations of Ti-O-Ti bond of [TiO<sub>6</sub>] octahedral [16, 17]. It is seen from Fig. 5 that initially in composite C1 having 20 wt% TiO<sub>2</sub> the band at 685 cm<sup>-1</sup> of ZBIB glass undergoes pronounced change and takes almost the similar shape of TiO<sub>2</sub> (compare curves b and g). However, with decreasing TiO<sub>2</sub> filler in the composites C2 to C4, this band undergoes a gradual change and the bands related to TiO<sub>2</sub> filler at 654 and 546 cm<sup>-1</sup> gradually become less intense (see Fig. 5, curve b-e). This fact clearly indicates the formation of Ti-O-Bi bonds (see Fig. 5 curve b) in the microcomposite dielectrics. In addition to this, the 923 cm<sup>-1</sup> band undergoes changes with formations of medium intense band at around 1023 and 908 cm<sup>-1</sup> which are due to asymmetric vibration of B-O-Si and B-O-Ti bonds [18] respectively. All the facts clearly indicate the distinct interaction of ZBIB glass with TiO<sub>2</sub> and SiO<sub>2</sub> fillers. It is seen from Fig. 5 by comparing spectra a-g that the nature of the spectra (b-e) of microcomposite dielectrics due to combined TiO<sub>2</sub>-SiO<sub>2</sub> addition gradually becomes closer to the individual filler at its respective highest content but has the mixed nature at their intermediate content. It further indicates that both the fillers have partially dissolved in the glass leaving behind residual fillers in the resultant microcomposite dielectrics. This is analogous to the observation of XRD as well as microstructural analysis discussed earlier.

### 3.5 Softening point and glass transition temperature

The softening point ( $T_s$ ) and glass transition temperature ( $T_g$ ) gradually increase as the  $\text{SiO}_2$  content in the combined  $\text{SiO}_2$ - $\text{TiO}_2$  filler increases from 5 to 20 wt%. But the effect is more pronounced on  $T_s$  than that on  $T_g$ . These facts are depicted in Figs. 6 and 7 respectively. A similar increasing trend of glass transition temperature with increasing  $\text{SiO}_2$  content has been demonstrated by Vernacotola and Shelby [19, 20] for potassium niobium silicate glasses. The increase of  $T_s$  and  $T_g$  is due to high melting points of  $\text{SiO}_2$  (1723°C) filler. It is also seen from Fig. 6 that  $\text{SiO}_2$  filler has greater effect on softening point as compared to  $\text{TiO}_2$  filler. This is due to higher electronegativity of Si (1.8) than Ti (1.5) which results in higher covalent character of the ultimate microcomposite dielectrics with increasing  $\text{SiO}_2$  content.

The extent of covalent bonding character of the resultant microcomposite dielectrics can be calculated approximately using the following formula [21]

$$\text{Covalent character (\%)} = \exp [-0.25 (\Delta\chi)^2] \times 100 \quad (1)$$

where  $\Delta\chi$  is the electronegativity of the composite, that is, the electronegativity difference ( $\chi_A - \chi_C$ ) of the anions and the cations. The average electronegativity of the anions ( $\chi_A$ ) or cations ( $\chi_C$ ) can be evaluated by the following simple additive relation [22]

$$\chi_A \text{ or } \chi_C = \sum N_i \chi_i / \sum N_i \quad (2)$$

where  $N_i$  and  $\chi_i$  are the number of individual constituent atom per mole and its electronegativity, respectively.

The variation of softening point,  $T_s$  and glass transition temperature,  $T_g$  of microcomposite dielectrics C1-C4 as a function of their covalent character is shown in Fig. 8. It is seen that both  $T_s$  and  $T_g$  increase with increase in covalent character of the

microcomposite dielectrics. Thus, there exists a direct relation between the  $T_s$  or  $T_g$  and covalent character of the microcomposite dielectrics, and seems to be regulated these properties. It is well known that covalent bond is stronger than ionic bond. Thus with increase in covalent character, the matrix of the microcomposite dielectric would be more strengthened. In consequence, their  $T_s$  and  $T_g$  would increase.

### **3.6 Coefficient of thermal expansion**

Variation of coefficient of thermal expansion (CTE) as a function of added  $TiO_2$  or  $SiO_2$  filler content is shown in Fig. 9. The CTE of composites gradually decreases as  $SiO_2$  filler content increases from 5 to 20 wt%. Vernacotola and Shelby [19, 20] have also found a similar decreasing trend of CTE with increasing  $SiO_2$  content in potassium niobium silicate glasses. It is well known that  $SiO_2$  filler has very low CTE ( $5.5 \times 10^{-7}/K$ ) as compared to the glass ( $82 \times 10^{-7}/K$ ) and  $TiO_2$  ( $80-100 \times 10^{-7}/K$ ). The resultant CTE of the microcomposite dielectrics, therefore, decreases gradually.

The above fact can also be well understood from the decrease in CTE with increase in covalent character of the composites which results in strengthening of connectivity of the network of composites. This is shown in Fig. 10. Thus, there exists an inverse relation between the CTE and covalent character of the microcomposite dielectrics. The matrix of the microcomposites would be strengthened with increase in covalent character.

Consequently, their CTE would increase.

### 3.7 Dielectric constant

Dielectric constants ( $\epsilon_r$ ) of the microcomposite dielectrics have been calculated by using the following formula<sup>23</sup>

$$\epsilon_r = cd/(0.0885 A) \quad (3)$$

where c, d and A are capacitance in pico Farad (pF), thickness of glass or microcomposite (in cm) and area of the dielectric (in cm<sup>2</sup>) respectively.

Variation of dielectric constant as a function of added TiO<sub>2</sub> or SiO<sub>2</sub> fillers is shown in Fig. 11. It is seen that the dielectric constant of the composites gradually decreases with increase in SiO<sub>2</sub> filler content. It is a well known fact that the dielectric constant of SiO<sub>2</sub> filler is 3.8 which is lower than that of the glass (11.2) whereas the dielectric constant of TiO<sub>2</sub> filler is higher (80-100) than the glass. Thus, the resultant dielectric constant of combined TiO<sub>2</sub>-SiO<sub>2</sub> filler added composite gradually decreases with increasing SiO<sub>2</sub> content or decreasing TiO<sub>2</sub> content. The variation of dielectric constant of composites C1-C4 as a function of their covalent character is already shown in Fig. 10. It is seen that the dielectric constants of the microcomposite dielectrics decrease with increase in their covalent character. Thus, there exists an inverse relation between the dielectric constant and the covalent character of the microcomposite dielectrics.

## 4 Conclusions

In this effort to disclose a lead-free environmental-friendly alternative microcomposite dielectric for the white back (rear glass dielectric layer) of plasma display panels, the co-effect of two types of TiO<sub>2</sub>-SiO<sub>2</sub> ceramic fillers to an extent of 25 wt% on the softening point, glass transition temperature, coefficient of thermal expansion and dielectric

properties of a new lead-free environmental-friendly ZnO-Bi<sub>2</sub>O<sub>3</sub>-B<sub>2</sub>O<sub>3</sub> (ZBIB) glass system has been investigated. Based on qualitative XRD and FTIR spectral analyses, both the fillers investigated are found to be partially dissolved in the glass at the sintering temperature (560°C), and thus the specimen successfully formed ceramic filler particulate-reinforced glass matrix microcomposites with a strong interfacial bonding. This is supported by the SEM images of the microcomposite dielectrics. The softening point, T<sub>s</sub> and glass transition temperature, T<sub>g</sub> have been found to be increased whereas coefficient of thermal expansion (CTE) and dielectric constant, ε<sub>r</sub> decreased with increasing SiO<sub>2</sub> content. The increase and decrease of these properties are correlated well with the covalent character (a fundamental property) of the resultant microcomposite dielectrics. The co-addition of TiO<sub>2</sub>-SiO<sub>2</sub> filler to ZBIB is found to be more effective in consideration of the desired properties of white back (the rear glass substrate) of the PDPs.

**Acknowledgements** This work has been supported by the NMITLI/CSIR, New Delhi under the sanctioned no. 5/258/49/2006-NMITLI. The authors gratefully thank Director of the institute for his kind permission to publish this paper. They also thankfully acknowledge the XRD, SEM and Ceramic Membrane Divisions of this institute for their respective help.

## References

1. J. S. An, J. S. Park, J. R. Kim, K. S. Hong, H. Shin, *J. Am. Ceram. Soc.*, **89**, 3658 (2006).
2. H. Shin, S. G. Kim, J. S. Park, J. S. An, K. S. Hong, H. Kim, *J. Am. Ceram. Soc.*, **89**, 3258 (2006).
3. R. R. Tummala, *Borate Glasses: Structure, Properties and Applications*, edited by L. D. Pye, et.al., Plenum Publishing Corp., 1978.
4. S. G. Kim, J. S. Park, J. S. An, K. S. Hong, H. Shin, H. Kim, *J. Am. Ceram. Soc.*, **89**, 902 (2006).
5. E. S. Lim, B. S. Kim, J. H. Lee, J. J. Kim, *J. Electroceram.*, **17**, 359 (2006).
6. S. G. Kim, H. Shin, J. S. Park, K. S. Hong, H. Kim, *J. Electroceram.*, **15**, 129 (2005).
7. C. L. Yawa, *Chemical Properties Handbook: Physical, Thermodynamic, Environmental, Transport, Safety and Health Related Properties for Organic and Inorganic Chemicals*, pp. 613-615, McGraw-Hill Book Co., New York, 1999.
8. E. Chong, S. Hwang, W. Sung, H. Kim, H. Shin, *Int. J. Appl. Ceram. Technol.*, **6**, 295 (2009).
9. E. Chong, S. Hwang, W. Sung, H. Kim, H. Shin, *Int. J. Thermophys.*, DOI 10.1007/s10765-008-0496-8.
10. M. B. Volf, *Chemical Approach to Glass*, p. 443, Elsevier Science Publishing Company, Inc., New York, 1984.
11. G. Fuxi, *Optical and Spectroscopic Properties of Glass*, pp. 18-61, Springer-Verlag, Berlin, 1992.

12. E. I. Kamitsos, A. M. Karakassides, D. G. Chryssikos, *J. Phys. Chem.*, **91**, 1073 (1987).
13. S. G. Motke, S. P. Yowale, S. S. Yawale, *Bull. Mater. Sci.*, **25**, 75 (2002).
14. L. Baia, R. Stefan, J. Popp, S. Simon, W. Keifer, *J. Non-Cryst. Solids*, **324**, 109 (2003).
15. A. A. Kharlamov, R. M. Almeida, J. Heo, *J. Non-cryst. Solids*, **202**, 233 (1996).
16. A. Shaim, M. Et-tabirou, M. Montagne, G. Palavit, *Mater. Res. Bull.*, **37**, 2459 (2002).
17. J. Rocha and M. W. Anderson, *Eur. J. Inorg. Chem.* **2000**, 801 (2000).
18. T. Uma, M. Nogami, *J. Phys. Chem. C.*, **111**, 16635 (2007).
19. D. E. Vernacotola, *Key Engg. Mater.*, **94-95**, 379 (1994).
20. D. E. Vernacotola, J. E. Shelby, *Phys. Chem. Glasses*, **35**, 53 (1994).
21. L. Pauling, *The Nature of the Chemical Bond*, 3rd edition, pp. 34-75, Cornell University Press, New York, 1960.
22. B. Karmakar, *J. Solid State Chem.*, **178**, 2663 (2005).
23. T. K. Dakin, *Standard Handbook for Electrical Engineers*, eds. D. G. Fink, & H. W. Beaty, 13<sup>th</sup> edition, McGraw Hill Inc., New York, pp. 4-117, 1993.

## Figure captions

Fig. 1 Particle size distribution of ZBIB glass powder, TiO<sub>2</sub> and SiO<sub>2</sub> fillers.

Fig. 2 Variation of XRD patterns with TiO<sub>2</sub> and SiO<sub>2</sub> filler content: (a) glass, G, (b) C1, (c) C2, (d) C3, and (e) C4 (for composition see Table 1). XRD patterns of added (f) SiO<sub>2</sub> and (g) TiO<sub>2</sub> fillers are also provided for comparison.

Fig. 3 SEM images after etching in HF of (a) C1 and (b) C4 (for composition see Table 1).

Fig. 4 Variation bulk density as a function of added TiO<sub>2</sub> or SiO<sub>2</sub> filler of composites C1-C4 (for composition see Table 1).

Fig. 5 FTIR spectra of (a) glass, G, (b) C1, (c) C2, (d) C3 and (e) C4 (for composition see Table 1). Spectra of added (f) SiO<sub>2</sub> and (g) TiO<sub>2</sub> fillers are also given for comparison.

Fig. 6 Variation of softening points, T<sub>s</sub> as a function of added TiO<sub>2</sub> or SiO<sub>2</sub> filler of composites C1-C4 (for composition see Table 1).

Fig. 7 Variation of glass transition temperature, T<sub>g</sub> as a function of added TiO<sub>2</sub> or SiO<sub>2</sub> filler of composites C1-C4 (for composition see Table 1).

Fig. 8 Variation of softening point, T<sub>s</sub> and glass transition temperature, T<sub>g</sub> of composites C1-C4 (for composition see Table 1) as a function of their covalent character.

Fig. 9 Variation of coefficient of thermal expansion (CTE) as a function of added  $\text{TiO}_2$  or  $\text{SiO}_2$  filler of composites C1-C4 (for composition see Table 1).

Fig. 10 Variation of coefficient of thermal expansion (CTE) and dielectric constant ( $\epsilon_r$ ) of composites C1-C4 (for composition see Table 1) as a function of their covalent character.

Fig. 11 Variation of dielectric constant ( $\epsilon_r$ ) as a function of added  $\text{TiO}_2$  or  $\text{SiO}_2$  filler of composites C1-C4 (for composition see Table 1).

**Table 1 Composition of microcomposite dielectrics derived from glass**

<b>Sample identity</b>	<b>Composition (wt%)</b>		
	<b>ZBIB glass</b>	<b>Added TiO<sub>2</sub> filler</b>	<b>Added SiO<sub>2</sub> filler</b>
G <sup>a</sup>	100	-	-
C1	75	20	5
C2	75	15	10
C3	75	10	15
C4	75	5	20

<sup>a</sup>Composition (wt %) of glass (G): 19ZnO-46 Bi<sub>2</sub>O<sub>3</sub>-35 B<sub>2</sub>O<sub>3</sub>

## Figures

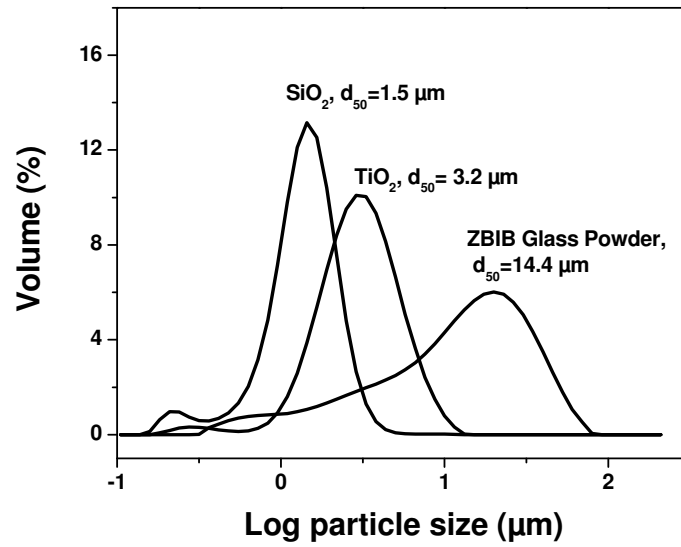


Fig. 1 Particle size distribution of ZBIB glass powder, TiO<sub>2</sub> and SiO<sub>2</sub> fillers.

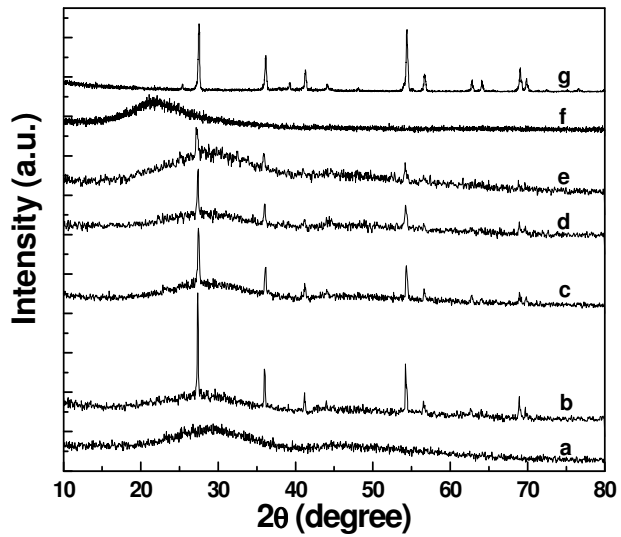


Fig. 2 Variation of XRD patterns with  $\text{TiO}_2$  and  $\text{SiO}_2$  filler content: (a) glass, G, (b) C1, (c) C2, (d) C3, and (e) C4 (for composition see Table 1). XRD patterns of added (f)  $\text{SiO}_2$  and (g)  $\text{TiO}_2$  fillers are also provided for comparison.

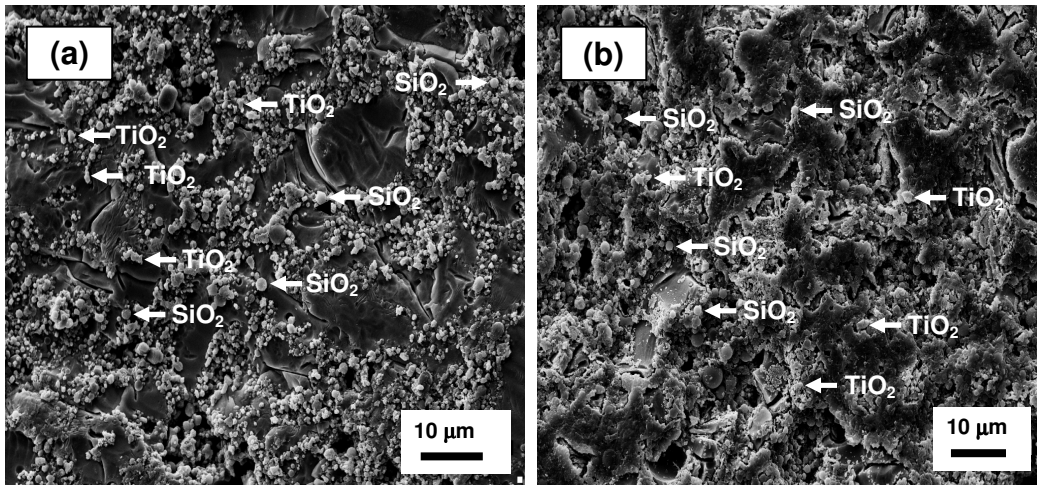


Fig. 3 SEM images after etching in HF of (a) C1 and (b) C4 (for composition see Table 1).

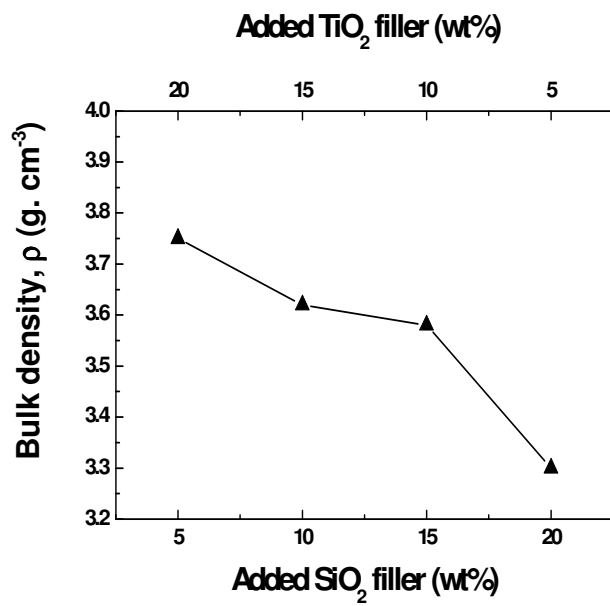


Fig. 4 Variation bulk density as a function of added  $\text{TiO}_2$  or  $\text{SiO}_2$  filler of composites C1-C4 (for composition see Table 1).

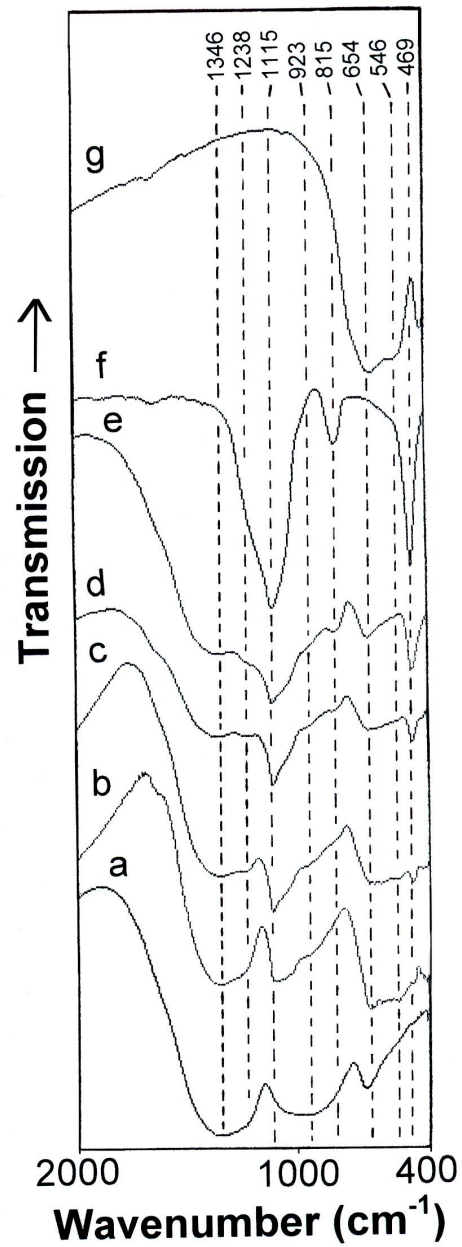


Fig. 5 FTIR spectra of (a) glass, G, (b) C1, (c) C2, (d) C3 and (e) C4 (for composition see Table 1). Spectra of added (f)  $\text{SiO}_2$  and (g)  $\text{TiO}_2$  fillers are also given for comparison.

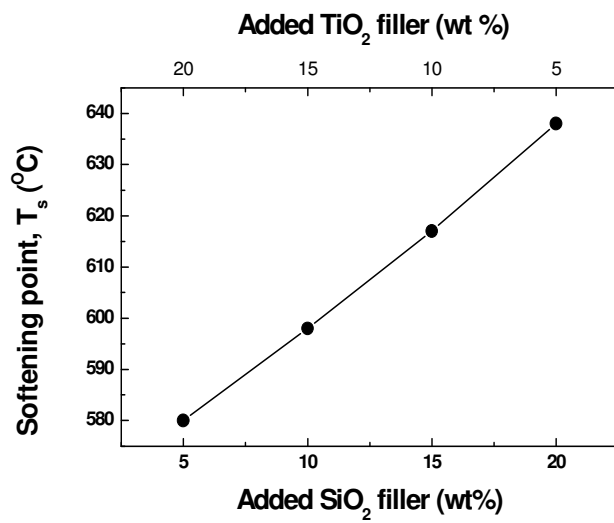


Fig. 6 Variation of softening points,  $T_s$  as a function of added TiO<sub>2</sub> or SiO<sub>2</sub> filler of composites C1-C4 (for composition see Table 1).

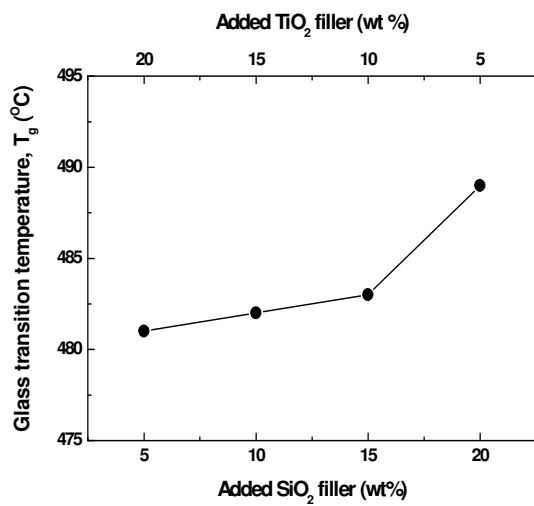


Fig. 7 Variation of glass transition temperature,  $T_g$  as a function of added  $\text{TiO}_2$  or  $\text{SiO}_2$  filler of composites C1-C4 (for composition see Table 1).

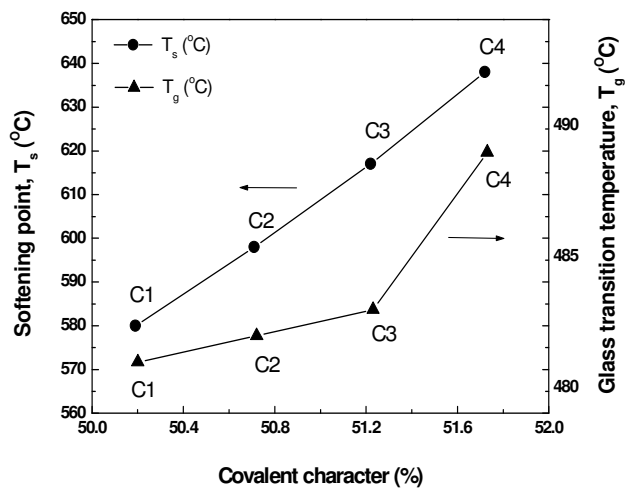


Fig. 8 Variation of softening point,  $T_s$  and glass transition temperature,  $T_g$  of composites C1-C4 (for composition see Table 1) as a function of their covalent character.

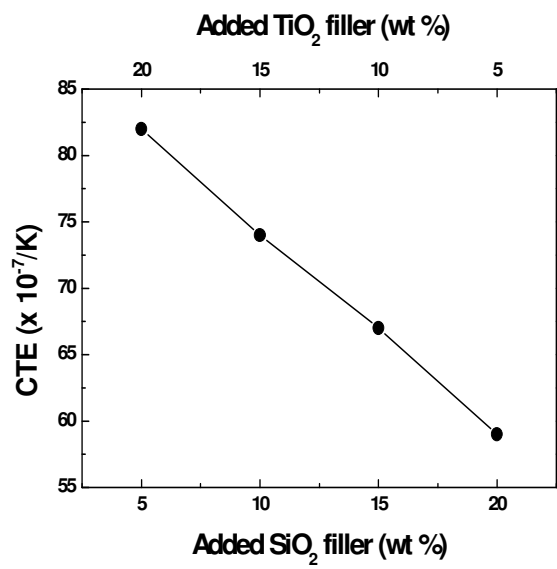


Fig. 9 Variation of coefficient of thermal expansion (CTE) as a function of added  $TiO_2$  or  $SiO_2$  filler of composites C1-C4 (for composition see Table 1).

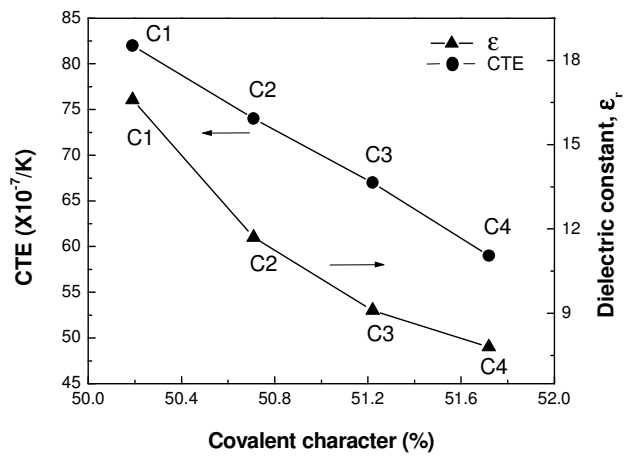


Fig. 10 Variation of coefficient of thermal expansion (CTE) and dielectric constant ( $\epsilon_r$ ) of composites C1-C4 (for composition see Table 1) as a function of their covalent character.

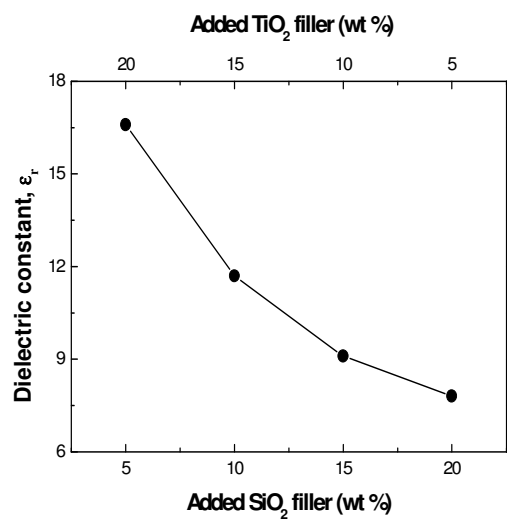


Fig. 11 Variation of dielectric constant ( $\epsilon_r$ ) as a function of added TiO<sub>2</sub> or SiO<sub>2</sub> filler of composites C1-C4 (for composition see Table 1).